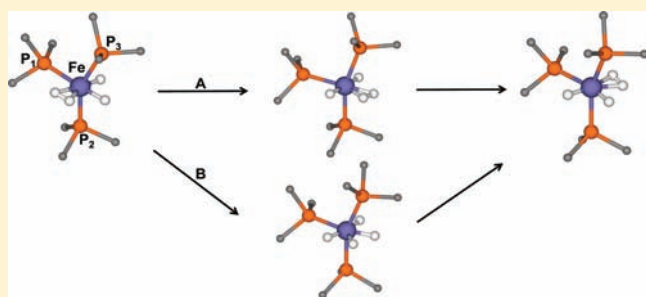


Fluxionality of Hydrogen Ligands in $\text{Fe}(\text{H})_2(\text{H}_2)(\text{PEtPh}_2)_3$ Nađa Došlić,[†] Vjeran Gomzi,[†] Momir Mališ,[†] Ivana Matanović,[†] and Juergen Eckert^{*‡}[†]Department of Physical Chemistry, Ruđer Bošković Institute, Bijenička 54, 10000 Zagreb, Croatia[‡]Materials Research Laboratory, University of California, Santa Barbara, California 93106, United States

ABSTRACT: Extensive computational investigations along with additional quasielastic neutron scattering data were used to obtain a consistent picture of the extensive fluxionality of hydride and dihydrogen ligands in $\text{Fe}(\text{H})_2(\text{H}_2)(\text{PEtPh}_2)_3$ over a wide range of temperatures from 1.5 to 320 K. We were able to identify three different regimes in the dynamical processes based on activation energies obtained from line spectral broadening. The rotational tunneling lines (coherent exchange of the two hydrogens of the H_2 ligand) are broadened with increasing temperature by incoherent exchange up to about 80 K at which point they merge into a quasielastic spectrum from 100 K to about 225 K. The effective activation energies for the two regions are 0.14 and 0.1 kcal mol⁻¹, respectively. A third dynamical process with a higher activation energy of 0.44 kcal mol⁻¹ dominates above 225 K, which we attribute to a quantum dynamical exchange of dihydrogen and hydride ligands. Our detailed density functional theory (DFT) structural calculations involving the three functionals (B3LYP, TPSS, and wB97XD) provide a good account of the experimental structure and rotational barriers when only the hydrogen ligands are relaxed. Full relaxation of the “gas-phase” molecule, however, appears to occur to a greater degree than what is possible in the crystal structure. The classical dihydrogen-hydride exchange path involves a cis-dihydrogen and tetrahydride structure with energies of 6.49 and 7.38 kcal mol⁻¹, respectively. Experimental observation of this process with much lower energies would seem to suggest involvement of translational tunneling in addition to the rotational tunneling. Dynamics of this type may be presumed to be important in hydrogen spillover from metal particles, and therefore need to be elucidated in an effort to utilize this phenomenon.



INTRODUCTION

The discovery that molecular hydrogen can form a sigma complex with transition metals by Kubas et al. in 1984¹ has been widely regarded as one of the most important, fundamental developments in Inorganic Chemistry in the last two decades of the 20th century. The importance of this type of binding for H_2 has increased dramatically in recent years because of the necessity to increase binding energies for molecular hydrogen in porous materials beyond those offered by simple physisorption,^{2–4} if this approach is to become a viable hydrogen storage medium at ambient temperatures.^{4–11} A significant increase of hydrogen storage capacities for sorption based systems at room temperature and modest pressures have recently been achieved by the so-called hydrogen spillover mechanism.^{12–16} In this approach small metal particles are introduced on or in high-surface area materials (e.g., carbons, IRMOF-8), which act to dissociate the hydrogen molecules under saturation conditions.^{17–19} In this situation atomic H is formed, which can then migrate into the support, and store in much higher quantity than H_2 because of its much smaller size. A crucial step in this sorption/desorption reaction at the metal particle involves a dynamic exchange between H_2 and H. This type of exchange has also been observed in transition metal polyhydride complexes,^{20,21} where the details can be studied much more readily as crystal structures of many of these complexes are known.^{1,22–24} Dihydrogen-hydride exchange reactions in metal complexes, which contain one or more hydride ligands along with coordinated dihydrogen, are readily

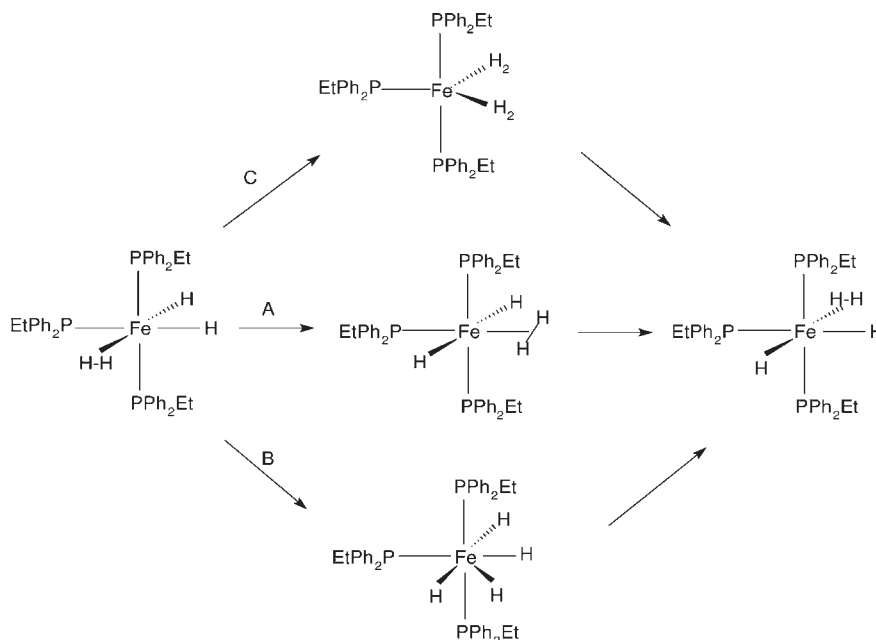
observed by NMR with the use of partial H/D substitution. Barriers to this process have been found to be generally somewhat higher than those for H_2 rotation,^{25–27} but in some cases can be very close to the latter.²⁸

In this work we investigate the quantum rotation of the H_2 and the dihydrogen-hydride exchange mechanism in the polyhydride compound $\text{Fe}(\text{H})_2(\text{H}_2)(\text{PEtPh}_2)_3$ by inelastic and quasielastic neutron scattering and electronic structure calculations. Possible structures (Scheme 1) involved in these processes include three dihydrogen-dihydride configurations (-cis, -trans, -meta) as well as the tetrahydride and bis-dihydrogen forms. Except for the latter, all of these were obtained in our structural calculations, and their energetics determined. What is known from an experimental point of view²³ is (1) that there is just one hydrogen signal in the NMR spectrum down to 183 K, that is, that the hydride and dihydrogen ligands are indistinguishable, and hence are exchanging rapidly, and for that reason it was impossible to determine the H-D coupling constant for an HD ligand, and (2) that the reorientation of the dihydrogen ligands occurs by rotational tunneling. The exchange processes shown would normally be expected to occur classically by way of transition states, although these were found to be rather high in energy in previous theoretical studies.^{23,29}

Received: June 10, 2011

Published: October 03, 2011

Scheme 1



A rather complete account of the structural as well as some dynamical properties of the $\text{Fe}(\text{H})_2(\text{H}_2)(\text{PEtPh}_2)_3$ complex to be investigated in this work have been reported.²³ Inelastic neutron scattering (INS) studies in this work were used to obtain information on the rotational potential energy surface (PES) by an empirical approach using planar rotation of the dihydrogen molecule fitted to observed rotational transitions. From the ground state rotational tunneling splitting of 6.4 cm^{-1} a barrier to H_2 rotation of $1.1 \text{ kcal mol}^{-1}$ was deduced. Theoretical analyses were, however, limited to model systems in which the phosphine ligands were replaced by PH_3 and to the use of extended Hückel calculations. Nonetheless the computations demonstrate the existence of a cis-effect, an attractive interaction of iron-hydride bond σ orbital and the unoccupied σ_{HH}^* orbital of dihydrogen ligand. This unique effect is thought to be responsible for the staggered dihydrogen conformation with respect to normal octahedral iron coordination, and may be instrumental in dihydrogen-hydride exchange in this material. The theoretical results were reconsidered two years later by Eisenstein and co-workers.²⁹ On the basis of more sophisticated multiconfigurational self-consistent field (MCSCF) calculations they found that the staggered dihydrogen conformation arises from a dipole/induced-dipole interaction in the crystal structure geometry.

Herein we go beyond the previous model system calculations and provide high level theoretical analyses of the structural and energetic properties of $\text{Fe}(\text{H})_2(\text{H}_2)(\text{PEtPh}_2)_3$ including dihydrogen rotation and dihydrogen-hydride exchange, in an effort to see if improved computations could achieve better agreement with experimental results, and point the way toward an understanding of the observed fluxionality of the hydrogen ligands at higher temperatures, especially that of the dihydrogen-hydride exchange. On the experimental side we report new quasielastic neutron scattering data on the dihydrogen and dihydrogen-hydride dynamics at temperatures from 150 to 320 K, which provide evidence of more complex dynamical behavior than previously thought.

■ QUASIELASTIC NEUTRON SCATTERING

Quasielastic neutron scattering (QENS) experiments were carried out on the IN6 time-of-flight neutron spectrometer at the Institute Laue-Langevin in Grenoble (France) at temperatures up to 320 K with an incident neutron wavelength of 5.1 \AA . The experiments are an extension of those reported in ref 23 which included a study of the temperature dependence of the rotational tunneling spectra. The rotational tunneling peaks were found to broaden appreciably with increasing temperature, and become essentially indistinguishable from an equivalent quasielastic line at about 110 K. One can define an effective activation energy for the temperature dependence of the broadening of the rotational tunneling lines by an Arrhenius relationship. This effective activation energy was found to be $0.10 \text{ kcal mol}^{-1}$ or 35 cm^{-1} . Broadening, as well as line shifts of the rotational tunneling lines with temperature have been attributed to a coupling to the phonon spectrum of the material³⁰ and to the transition to the first excited librational state,³¹ which in the present case is far greater, that is, 170 cm^{-1} , than this activation energy, contrary to the expectation of these models.

Here we report additional quasielastic neutron scattering data at temperatures of 150, 175, 200, 225, 250, 300, and 320 K whose initial aim was to observe the temperature dependent evolution of the rotational dynamics of the dihydrogen ligand. The sample appeared to be stable at 320 K, which was the highest temperature that could be reached with the cryostat used. The Lorentzian linewidths of the quasielastic scattering spectra summed over all scattering angles were obtained by convolution of the measured instrumental energy resolution function with a single Lorentzian whose parameters were fitted to the experimental data in the process (Figure 1). The resulting widths are shown on a semilog plot (Figure 2) vs reciprocal temperature to display the likely Arrhenius behavior of the temperature dependence of the dynamics. This figure also includes the aforementioned change in the width of the rotational tunneling lines with temperature, as well as the quasielastic widths of a Ru analogue with no

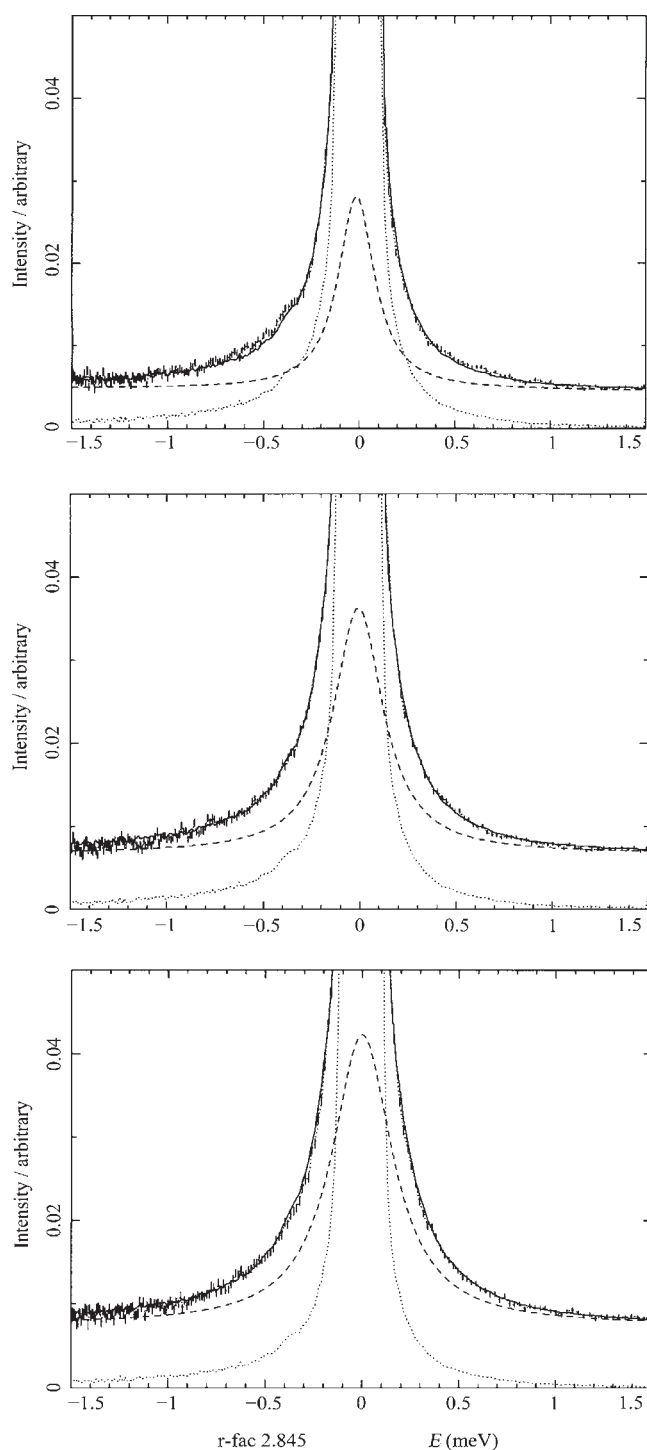


Figure 1. Quasielastic neutron scattering spectra at $T = 150$, 250 , and 320 K.

dihydrogen ligand, namely, $\text{RuH}_4(\text{PPh}_3)_3$ for reasons to be discussed below. It is immediately apparent, however, that the widths fall into three different regimes as a function of temperature: the slope below $T \approx 225$ K is similar to that for the broadening of the rotational tunneling lines (below 80 K) but in turn is appreciably less than that at higher temperatures. Activation energies of $0.14 \text{ kcal mol}^{-1}$ and $0.44 \text{ kcal mol}^{-1}$, respectively, were obtained by fitting the Arrhenius relationship to the

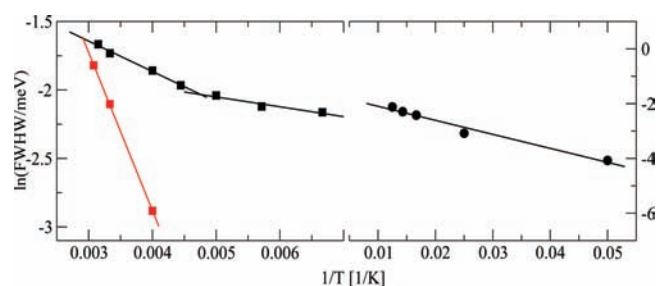


Figure 2. Right: \ln of the width of a rotation tunneling line as a function of $1/T$; Left: \ln of the width of a quasielastic lines as a function of $1/T$. Black, $\text{Fe}(\text{H})_2(\text{H}_2)(\text{PEtPh}_2)_3$ complex; red, $\text{RuH}_4(\text{PPh}_3)_3$ complex.

latter two regimes. The value obtained at lower temperatures is nearly the same as the one derived from the temperature dependence of the width of the rotational tunneling peaks up to 110 K, and may therefore be attributed to the same process described above. We note, however, that this type of spectral change from discrete tunneling lines to a quasielastic spectrum has, in the past, been attributed by some authors²⁹ to a “transition” to a (semi)classical regime, where higher energy states become accessible by hopping over the barrier, or thermally activated reorientation. The barrier to rotation determined in the previous experiment of $1.1 \text{ kcal mol}^{-1}$ ($\approx 560 \text{ K}$) is, however, much too high for this process to be significant at the temperatures of this experiment. A different description of this temperature dependence was given by Limbach and coworkers³² in terms of different activation energies for the coherent exchange (the rotational tunneling regime at low temperatures) and an incoherent exchange of the two H's at higher temperatures. None of these descriptions do, however, include yet another change in the dynamics at still higher temperatures as observed by us above 225 K, where the broadening of the quasielastic line is governed by a higher activation energy of $0.44 \text{ kcal mol}^{-1}$. The origin of this additional dynamic process would seem to lie in the interaction between the dihydrogen ligand and the adjacent hydrides, the equivalent of which does not exist in the case of the methyl group rotation, which is the subject of most of the theories referred to above. In fact, in an earlier study of quasielastic broadening at high temperatures in the compound $\text{IrClH}_2(\text{H}_2)(\text{P-}i\text{-Pr}_3)_2$ Li et al. were able to identify a similar high temperature process with an activation energy of $1.5 \text{ kcal mol}^{-1}$ as one involving a dynamic dihydrogen-hydride exchange. This conclusion was supported by extensive computational studies which demonstrated that energy differences between the respective configuration were of similar magnitude as the experimental activation energy.

THEORETICAL BACKGROUND

Calculations were performed using density functional theory (DFT). We tested several density functionals for their ability to reproduce the experimental staggered dihydrogen conformation and the barrier to H_2 rotation leading to the observed rotational tunneling splitting. We found that the wB97XD functional with long-range correlation and dispersion corrections^{33,34} gives a reliable account of the factors governing the dihydrogen rotation. Throughout the paper we compare the results with the conventional B3LYP^{35,36} and the meta-GGA TPSS³⁷ functionals. Effective core potentials (ECP) for iron and phosphorus atoms^{38–40} were used as part of the LanL2DZdp basis set.^{41,42} Several Gaussian basis sets were compared and 6-311G(d) was selected for all atoms except for

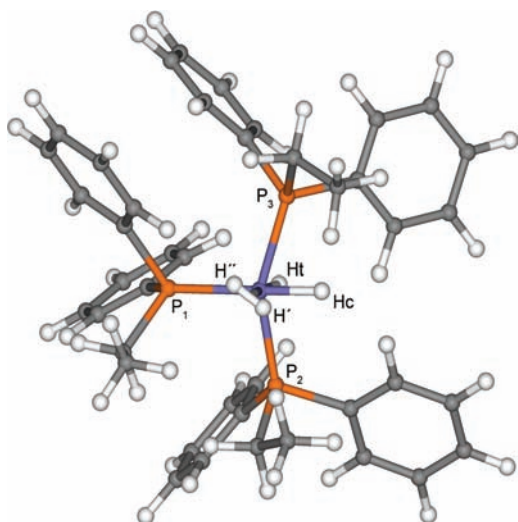


Figure 3. Structure of $\text{Fe}(\text{H})_2(\text{H}_2)(\text{PEtPh}_2)_3$ in the crystal as reported in ref 23.

the four hydrogens coordinated to the metal where the 6-311+G(d,p) was employed. All electronic structure calculations were performed with the Gaussian09 suite of programs⁴³ with the pruned (99590) grid (“ultrafine” grid) and the tight option for geometry optimization. Stationary points were validated by means of frequency calculations. Although $\text{Fe}(\text{H})_2(\text{H}_2)(\text{PEtPh}_2)_3$ is a system of paired electrons, the influence of higher spin orbital configurations on the H_2 rotation and dihydrogen/hydride exchange was also assessed by unrestricted DFT calculations. PESs for H_2 rotation were computed for the crystal structure as well as for the partially and fully optimized structures, and rotational energy levels were calculated on the 1D PESs using the spherical harmonics basis⁴⁴ and the Lanczos diagonalization algorithm^{45,46} as implemented in the ARPACK code.^{47,48}

RESULTS AND DISCUSSION

Rotational Dynamics of the Dihydrogen Ligand. The structure of $\text{Fe}(\text{H})_2(\text{H}_2)(\text{PEtPh}_2)_3$ in the crystal (Figure 3) as reported in ref 23 exhibits an obvious deviation from octahedral geometry. The P1-Fe-P2 and P1-Fe-P3 angles are larger than 90° and unequal, 97.6° and 105.2° , respectively. The P2-Fe-H_t and P3-Fe-H_t angles are smaller than 90° and almost equal (79.6°) so that the phosphines are bent toward the dihydrogen/hydride portion of the compound, but away from the dihydrogen. The equatorial planes $\text{H}_c\text{-H}_t\text{-P1}$ and $\text{Fe-H}_c\text{-H}_t$ planes are nearly identical. The Fe-H_c and Fe-H_t bonds are shorter than those to the dihydrogen and the H-H distance is 0.821 \AA . However, what makes $\text{Fe}(\text{H})_2(\text{H}_2)(\text{PEtPh}_2)_3$ unique is the fact that the dihydrogen bond is staggered with respect to all other bonds in the coordination sphere, that is, the Fe-H1-H2 plane is rotated by 43° with respect to the $\text{H}_c\text{-H}_t\text{-P1}$ plane.

The potential energy profiles for dihydrogen rotation in the $\text{Fe}(\text{H})_2(\text{H}_2)(\text{PEtPh}_2)_3$ as computed using the wB97XD (thin), B3LYP (bold), and TPSS (dashed) functionals are shown in the lower panel of Figure 4. The orientation of H_2 was varied in the interval $0^\circ < \theta < 180^\circ$ in steps of 10° while the remaining degrees of freedom were kept fixed at that of the crystal structure geometry. To facilitate the comparison with the paper of Van Der Sluys et al.,²³ the orientation of the dihydrogen is defined by the angle of a rotation, θ , with $\theta = 0^\circ$ corresponding to the

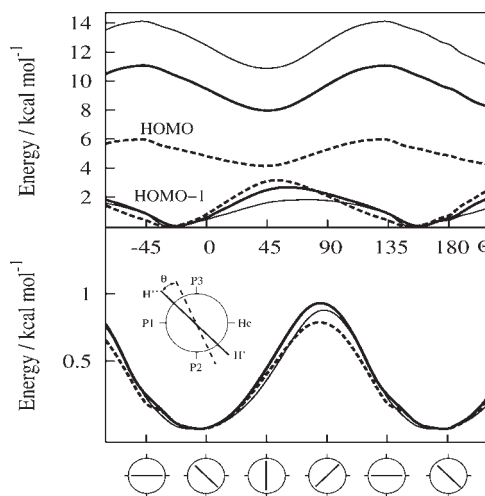


Figure 4. Lower panel: Potential energy curves (in kcal mol^{-1}) for H_2 rotation in the rigid $\text{Fe}(\text{H})_2(\text{H}_2)(\text{PEtPh}_2)_3$ obtained using the wB97XD (thin), B3LYP (bold), and TPSS (dashed) functionals. Upper panel: The corresponding HOMO and HOMO-1 orbital energies as function of the rotational angle θ . Inset: definition of the rotational angle θ .

experimental geometry as shown in the inset of Figure 4. The barrier to H_2 rotation is of the form of a simple double well potential, with barrier heights of $0.87 \text{ kcal mol}^{-1}$, $0.95 \text{ kcal mol}^{-1}$, and $0.79 \text{ kcal mol}^{-1}$ obtained with the use of the wB97XD, B3LYP, and TPSS functionals, respectively. In all cases the position of the minimum at $\theta \approx -4.0^\circ$ is in very good agreement with that of the experimental structure. Table 1 compiles the eigenvalues computed in the spherical harmonics basis $\psi_m = \exp(\pm im\theta)/(2\pi)$ with m up to 10. The ground state rotational tunneling splittings of 10.7 , 8.8 , and 12.3 cm^{-1} computed by using the three DFT methods agree fairly well with the observed value of 6.4 cm^{-1} given the fact that the tunneling transitions are extremely sensitive to the barrier height with an approximately exponential dependence. In the previous investigation²³ a barrier to H_2 rotation of $1.1 \text{ kcal mol}^{-1}$ was derived from the rotational ground state splitting by using the first two Fourier coefficients of the potential expansion

$$V = \sum_n V_{2n}(1 - \cos(2n\theta))/2 \quad (1)$$

The variation of the highest occupied molecular orbital (HOMO) and HOMO-1 orbital energies as function of the rotation angle θ is shown in the upper panel of Figure 4. It is apparent that the minimum of the HOMO occurs when the H-H axis eclipses the Fe-P2 and the Fe-P3 axes at $37^\circ < \theta < 57^\circ$, respectively. For these geometries the dihydrogen ligand is involved in π -backdonation with the HOMO, a hybrid of d_{yz} and d_{xy} located along these bonds. On the other hand, when the H-H axis eclipses the Fe-P1 axis the dihydrogen ligand is involved in π -backdonation with HOMO-1, the other combination of d_{yz} and d_{xy} . Because of the strong deviation of $\text{Fe}(\text{H})_2(\text{H}_2)(\text{PEtPh}_2)_3$ from the octahedral geometry the HOMO-1 orbital is not entirely perpendicular to the P2-Fe-P3 plane, but is tilted toward the P1-Fe-P3 region to avoid the more crowded P1-Fe-P2 quadrant. This is manifested in the asymmetry of the HOMO-1 energy profile. We note that the three functionals give considerably different HOMO/HOMO-1 gaps.

Table 1. Rotational Transitions (in cm^{-1}) for H_2 Rotation in the $\text{Fe}(\text{H})_2(\text{H}_2)(\text{PEtPh}_2)_3$ Crystal Structure^a

transition	experiment	wB97XD		B3LYP		TPSS	
		comp.	scaled (1.37)	comp.	scaled (1.28)	comp.	scaled (1.50)
0→1	6.4	10.7	6.4	8.8	6.4	12.3	6.4
0→2	170	148.4	185.8	155.4	187.9	139.1	187.0
0→3	252	223.6	241.7	228.4	244.1	222.2	245.6

^aThe transitions are given for the calculated rotational profile (comp.) and for the one in which the barrier to H_2 rotation is scaled to obtain the experimental ground state splitting (scaled). The scaling factor is given in brackets.

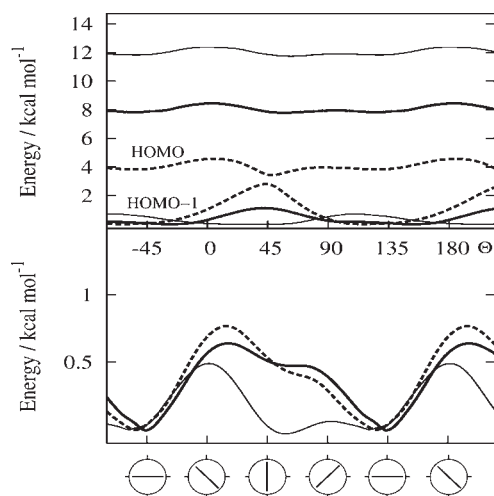


Figure 5. Lower panel: Potential energy curves (in kcal mol^{-1}) for H_2 rotation in the relaxed $\text{Fe}(\text{H})_2(\text{H}_2)(\text{PEtPh}_2)_3$ obtained using the wB97XD (thin), B3LYP (bold), and TPSS (dashed) functionals. Upper panel: The corresponding HOMO and HOMO-1 orbital energies as function of the rotational angle θ .

The nonhybrid TPSS functional predicts the smallest HOMO/HOMO-1 gap with the minimum of the sum of the two orbital energies at $\theta = -18.5^\circ$, while the largest difference in HOMO and HOMO-1 eigenvalues of $10.9 \text{ kcal mol}^{-1}$ is obtained with the wB97XD functional. This difference is expected as the HOMO eigenvalues predicted by nonhybrid functionals are generally less reliable than those predicted by hybrid functionals.⁴⁹ On the basis of these molecular orbital considerations alone the orientation of the dihydrogen should be in the P2–Fe–P3 plane, but it is also affected by electrostatic interactions. The molecular dipole moment of the complex gives rise to an induced dipole at the H_2 so that the most favorable orientation for the dihydrogen is to be parallel to this dipole moment vector. In $\text{Fe}(\text{H})_2(\text{H}_2)(\text{PEtPh}_2)_3$ the dipole moment of $\mu = 2.05D$ computed using the wB97XD method is directed toward the P1 ligand and encloses an angle of 49.6° with the H–H vector, that is, it lies almost in the equatorial plane. Hence the dipole/induced dipole interaction favors a conformation with H_2 approximately in the P1–H_r–H_c plane. The best balance between these interactions is therefore achieved for the observed staggered conformation. Because of the variety of interactions involved, small perturbations of the system geometry may well lead to changes in both the preferred orientation and the energy profile for the dihydrogen rotation.

We analyzed the H_2 rotation first for a partially and subsequently a fully optimized $\text{Fe}(\text{H})_2(\text{H}_2)(\text{PEtPh}_2)_3$. Even the partial optimization

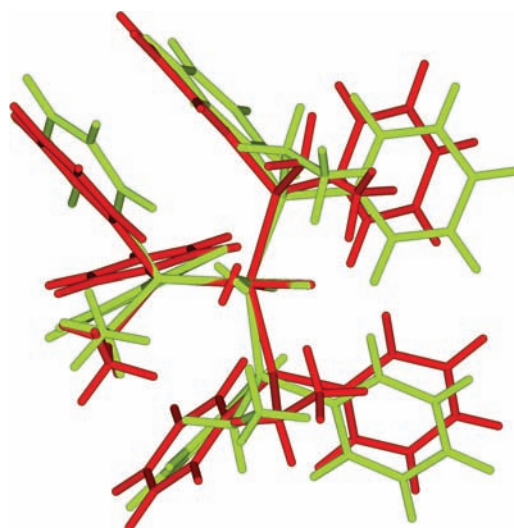


Figure 6. Superposition of the molecular structure in the crystal (green) and the computed wB97XD global minimum structure (red). The rmsd between the structures is 1.19 \AA .

of the dihydrogen along with the two hydride ligands leads to changes in the dihydrogen orientation. All three methods predict that the H–H bond is bent more toward the equatorial plane. For example, the B3LYP minimum is located at $\theta = -16.7^\circ$. The energy profiles for H_2 rotation for a fully relaxed $\text{Fe}(\text{H})_2(\text{H}_2)(\text{PEtPh}_2)_3$ are displayed in Figure 5. One immediately notices that this potential differs significantly from the rigid rotor situation. All three methods predict a minimum for a structure in which the H–H axis is lying in the equatorial plane. The wB97XD functional, however, predicts a second minimum, which in fact is the global minimum, at $\theta = 58.9^\circ$. In this structure the H–H axis eclipses the Fe–P3 bond. The energy difference between the two wB97XD minima is only $0.05 \text{ kcal mol}^{-1}$, and the two H_2 positions are separated by an energy barrier of $0.09 \text{ kcal mol}^{-1}$. The lowest energy levels of the H_2 are, however, well above this barrier. The global minima of this PES are separated by an energy barrier of $0.51 \text{ kcal mol}^{-1}$. In a similar vein the B3LYP and TPSS potentials clearly show a shoulder at $\theta \approx 60^\circ$. Changes of the HOMO and HOMO-1 eigenvalues along the rotation profile are shown in the upper panel of Figure 5. In all cases the variation of the HOMO is small indicating that the stabilization of the minima arises primarily from the interaction with HOMO-1. Note also that the dipole moment lies almost in the equatorial plane. The changes in the rotation profile are the result of sizable differences in the geometry of the molecular framework. The differences between our minimum energy structure obtained with the wB97XD method (red) and the experimental structure in the crystal are illustrated by a superposition of both them shown in Figure 6. The P1–Fe–P2 angle (104.2°) is

larger than P1–Fe–P3 (101.7°) in the fully optimized structure in contrast to the situation in the crystal, and the phosphine ligands are less bent toward H_t and the phenyl rings of the P1 and P3 ligands appear to be oriented in such a way to maximize the stacking interaction. The minimum energy orientation of the dihydrogen ligand in the fully optimized structure, however, deviates significantly from that in the experimental structure as described above for the rotational PESs. This result, as well as the relative lack of agreement of the rotational barrier heights of the fully relaxed potential energy curves with the experimental observations can, however, be qualitatively understood by noting that it is highly likely that Fe(H)₂(H₂)-(PEtPh₂)₃ in the crystal cannot relax as easily as our gas phase calculations allow on account of crystal packing forces and of considerable intermolecular interactions. This can easily be seen from an analysis of interatomic distances in the crystal structure, which has a number of short (less than the sum of the van der Waals radii) intermolecular contacts between phosphine H's of neighboring molecules. A calculation of the rotational potential energy curve should therefore include relaxation of neighboring molecules as well, but this task is currently prohibitive with close to 800 atoms in the unit cell.

We may interpret the observed temperature dependencies of the width of the rotational tunneling lines, and subsequent quasielastic broadening up to temperatures around 200 K in terms of a combination of a coherent exchange process (i.e., rotational tunneling) of the two H's of the dihydrogen ligand at low temperatures, and an incoherent, stochastic process at higher temperatures,³² where the latter is governed by a temperature dependent rate constant *k*. Both of these processes involve reorientations of the dihydrogen ligand, which is subject to quantum coherence of the initial and final states at low temperatures. This quantum coherence is gradually lost as temperature is increased and the reorientation assumes more of a stochastic, or incoherent character, which becomes the dominant source of the broadening of the quasielastic line at high temperatures. Two different activation energies can therefore be defined: one, which describes the coherent exchange of the two H's, and another for the incoherent exchange at higher temperatures. The temperature-dependent part of the width of the rotational tunneling lines is plotted on the right-hand side of Figure 2 up to 80 K, the highest temperature at which these lines are still distinct (Figure 2). This width contains a contribution for the coherent exchange, which is difficult to extract separately and taken to be only weakly temperature dependent,³² as well as that of the rate constant for incoherent exchange, which increases with temperature. The effective activation energy for this rate constant was found to be 0.10 kcal mol⁻¹. Above 100 K the INS spectra no longer exhibit tunneling lines but simply a quasielastic broadening for which we find an effective activation energy of 0.14 kcal mol⁻¹ up to about 225 K, which must mainly reflect the incoherent exchange process. This reason that this value is slightly greater than that of the tunneling lines at low temperature must be that the coherent exchange process (rotational tunneling) no longer contributes significantly at those temperatures.

This qualitative analysis does not specifically address the origin of the broadening and the related activation energies, which have, in the case of methyl rotation, been attributed to coupling with phonons and the excitation to the first excited librational state.³¹ In the case where this coupling is weak, the effective activation energy for broadening of the tunneling lines is expected to be the same as the energy of the librational excitation.⁵⁰ This simple

picture, however, does not seem to hold for metal dihydrogen complexes, where the librational transition is typically much greater than the activation energy derived from the broadening of the rotational tunneling lines. We have calculated the rotational energy levels (Table 1) for all the partially and fully relaxed rotational potential energy curves, and find that in no case lies the lowest librational level at a frequency of lower than 160 cm⁻¹ above the ground state after scaling the calculated transitions to the observed value of the ground state splitting of 6.4 cm⁻¹. Our results for the librational transitions are in good agreement with the observed²³ librational level at 170 cm⁻¹, and are far greater than the activation energy of 35 cm⁻¹ for broadening of the tunneling lines.

A different channel for the gradual loss of coherence in the reorientation of the dihydrogen ligand must therefore be in effect, which is likely to involve coupling of dihydrogen exchange to some low frequency skeletal deformation of the complex leading to a different reaction path. Indeed, among the frequencies calculated in the course of the structural minimizations described above we find a number of very low frequency deformation modes (11 to 42 cm⁻¹) of the Fe(H)₂(H₂)-(PEtPh₂)₃, which include displacements of the H atoms of the dihydrogen ligand, could therefore form part of the vibrational bath which leads to the broadening of the tunneling lines. A detailed mechanism was in fact worked out using quantum dynamics by Scheurer et al.⁵¹ for a much simpler case of pairwise exchange of two separate hydrides involving just two degrees of freedom, a metal-H bending mode, and the rotation of a dihydrogen intermediate. Here the damping of the tunneling system was in fact described by an interaction with a heat bath arising from the vibrational modes of the system.

Dihydrogen-Hydride Exchange. Rapid exchange of the dihydrogen and hydride ligands was clearly evident in the solution NMR spectrum²³ at temperatures as low as 183 K so that decoalescence of the hydride and dihydrogen signals could never be observed, nor was it possible to measure the H/D coupling constant in a sample with partially deuterated hydride ligands. This dihydrogen/hydride exchange is proposed to occur classically through a concerted rotation/bond-breaking mechanism at the cis-position.²³ We find, however, that the structure in which the dihydrogen is bound in the cis-position is between 5.16–6.49 kcal mol⁻¹ higher in energy, depending on the functional used. Similar, apparently high barriers (in the order of 5.8 kcal mol⁻¹ or greater) for such an exchange have been found in related systems, such as [Cp*OsH₄(PPh₃)]⁺,²⁴ but these are normally taken to be the energy of some calculated transition state. Experimental values for the dihydrogen-hydride exchange are an estimate, and are not determined directly in the NMR experiments. It is certainly possible, however, that translational tunneling of the hydrides could be involved in this process, as is frequently observed for proton transfer in a wide variety of systems.⁵² If this were the case, the dihydrogen-hydride exchange could occur much more rapidly, than the barrier indicated by the energy of a theoretical transition state. An indication of this possibility may be provided by the fact that we found that the optimized structure in which the dihydrogen is bound in the trans-position differs by only a small amount, namely, -0.09 kcal mol⁻¹ and 0.33 kcal mol⁻¹ using the B3LYP and TPSS functionals, respectively, and 1.95 kcal mol⁻¹ by using the dispersion corrected wB97XD functional from that of the global minimum structure, while the associated geometrical arrangements show appreciable differences in the gas phase calculations.

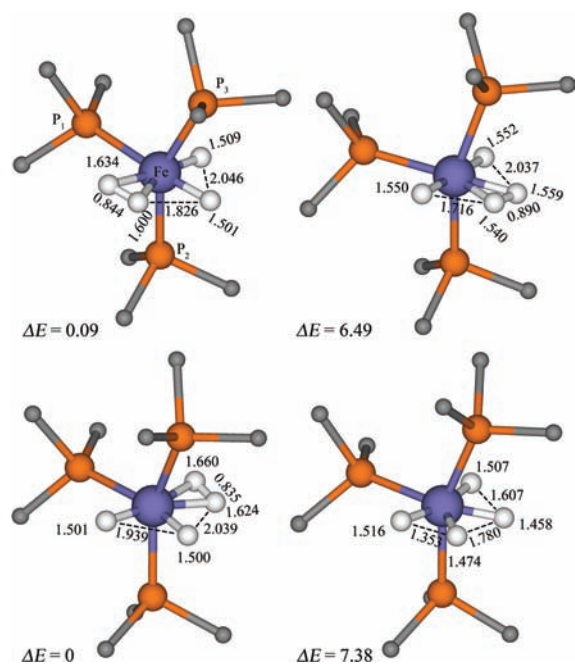


Figure 7. Geometries of the central part of $\text{Fe}(\text{H})_2(\text{H}_2)(\text{PEtPh}_2)_3$ for the two lowest energy structures, the global minimum with the dihydrogen axis lying in the equatorial plane (upper left), the trans configuration (lower left), as well as the cis-dihydrogen and tetrahydride intermediates, as calculated using B3LYP. Note that use of TPSS and wB97XD gives lower energies for global minimum structure than that of its trans-analogue. Note that strictly for graphical reasons the $(\text{PEtPh}_2)_3$ groups were replaced by $(\text{PH}_3)_3$.

We do in fact observe a third dynamical process (Figure 2) in the quasielastic neutron scattering spectra of $\text{Fe}(\text{H})_2(\text{H}_2)(\text{PEtPh}_2)_3$ at temperatures above approximately 225 K with activation energy of $0.44 \text{ kcal mol}^{-1}$, which we tentatively attribute to the dihydrogen-hydride exchange, despite the high energy of the likely classical intermediates. If this process involves translational tunneling the effective activation energy could be appreciably lower, and conceivable fall into the range given by this activation energy. We show, for comparison, the temperature dependence of the quasielastic broadening of the related Ru tetrahydride complex, $\text{RuH}_4(\text{PPh}_3)_3$, for which we find an activation energy of $2.29 \text{ kcal mol}^{-1}$. In this case the quasielastic broadening cannot arise predominantly from dihydrogen rotation only, as the dihydrogen-dihydride configuration can only be an intermediate in the exchange of the four separate hydrides. This in turn would be the reason for the higher activation energy than that for $\text{Fe}(\text{H})_2(\text{H}_2)(\text{PEtPh}_2)_3$, where the dihydrogen-dihydride forms are the two lowest energy structures. Other possible source of this high temperature broadening of the quasielastic line, such as classical stochastic reorientation of the phenyl or ethyl groups, can be ruled out because the activation energies required would be far too high.

The lack of agreement between our new calculated transition state energies and the observed activation energy attributed to dihydrogen-hydride exchange suggests that the latter must be treated by quantum dynamics and that translational tunneling of hydrides may well be involved. We note, for example, (Figure 7) that our calculated tetrahydride intermediate has two pairs of hydride ligands that are sufficiently close (1.607 and 1.353 Å, respectively) to facilitate the type of pairwise H/H exchange with the attendant formation of a dihydrogen intermediate described

by Scheurer et al.,⁵¹ one of which would end up being a stable structure. In fact, the pair of H's in the position on the tetrahydride where the dihydrogen is found in the global minimum structure would commonly be viewed as an "elongated dihydrogen ligand",²¹ and it may provide one of many pathways for rearrangements of hydride and dihydrogen ligands in this system.

To resolve issues of the actual reaction path of the dihydrogen hydride exchange, and the nature of the dynamics, including the possible involvement of translational tunneling in addition to the rotational tunneling of any dihydrogen intermediate, extensive ab initio molecular dynamics computations are required which take into account all the degrees of freedom. This was shown, for example, in the well-known case of CH_5^+ .⁵³ While ab initio molecular dynamics simulations are indeed now possible for systems of significant complexity, they depend critically on the availability of accurate electronic structure methods. The importance of an application of this approach in the case of transition metal polyhydrides, cannot be understated as it would lead to a much improved understanding of a considerable number of important reactions that effectively involve interconversion of dihydrogen and hydrides such as the before mentioned hydrogen spillover process.

CONCLUSIONS

We have carried out extensive computational and new experimental studies on the fluxionality of the hydrogen ligands in the polyhydride $\text{Fe}(\text{H})_2(\text{H}_2)(\text{PEtPh}_2)_3$. In accordance with earlier studies we found that the staggered conformation of H_2 is a consequence of a delicate balance between the back-donation from the metal d-orbitals and electrostatic interactions favoring the coplanarity of the H–H axis with the dipole moment vector. We have shown that this balance is strongly affected by structural relaxation of the dihydrogen complex. Non-Arrhenius behavior was observed for the broadening of the rotational tunneling lines along with subsequent broadening of the quasielastic line in the neutron scattering spectra over three different temperature regimes. These can be related to the reorientational dynamics of the H_2 dynamics, and provide a measure of the combined coherent and incoherent H/H exchange processes of the dihydrogen ligand as previously described.³² This very low activation energy for this broadening (35 cm^{-1}) makes it clear that it cannot be related to the excitation of the system to the higher librational state ($>160 \text{ cm}^{-1}$) but more likely to a coupling involving very low frequency deformations of the $\text{Fe}(\text{H})_2(\text{H}_2)(\text{PEtPh}_2)_3$. At temperatures above approximately 225 K we observe a third dynamical process with an activation energy of $0.44 \text{ kcal mol}^{-1}$, which we tentatively attribute to a nonclassical exchange between dihydrogen and hydride ligands, a process, which has to involve translational as well as rotational tunneling. Our calculations do indicate that the cis-effect put forward in the original paper is not likely to promote the classical dihydrogen/hydride exchange, since the structure in which the H_2 ligand is bound in the "cis-position" is $5.16\text{--}6.49 \text{ kcal mol}^{-1}$ higher in energy. We have, however, found that the structure with the dihydrogen ligand bound in the trans position may be relevant to dihydrogen/hydride exchange. The details of the reaction path mechanism including tunneling processes, however, remain to be elaborated.

AUTHOR INFORMATION

Corresponding Author

*E-mail: juergen.eckert@mrl.ucsb.edu.

ACKNOWLEDGMENT

This work has been supported by the MZOŠ project 098-0352851-2921. Work at UCSB was supported by a grant from the Office of Energy Efficiency and Renewable Energy, U.S. Department of Energy. Some of the computations were performed on POPLE at the Pittsburgh Supercomputing Center under a Teragrid startup request (CHE100052). We would also like to thank the Institut Laue-Langevin (Grenoble, France) for provision of beamtime for the neutron scattering experiments.

REFERENCES

- (1) Kubas, G. J.; Ryan, R. R.; Swanson, B. I.; Vergamini, P. J.; Wasserman, H. J. *J. Am. Chem. Soc.* **1984**, *106*, 451–452.
- (2) Rosi, N. L.; Eckert, J.; Eddaoudi, M.; Vodak, D.; Kim, J.; O’Keeffe, M.; Yaghi, O. *Science* **2003**, *300*, 1127.
- (3) Cote, A. P.; Benin, A. I.; Ockwig, N. W.; O’Keeffe, M.; Matzger, A. J.; Yaghi, O. M. *Science* **2005**, *310*, 1166.
- (4) Murray, L. J.; Dinca, M.; Long, J. R. *Chem. Soc. Rev.* **2009**, *38*, 1294.
- (5) Kubas, G. J. *J. Organomet. Chem.* **2009**, *694*, 2648–2653.
- (6) Bushnell, J. E.; Kemper, P. R.; van Koppen, P.; Bowers, M. T. *J. Phys. Chem. A* **2001**, *105*, 2216–2224.
- (7) Weck, P. F.; Kumar, T. J. D.; Kim, E.; Balakrishnan, N. *J. Chem. Phys.* **2007**, *126*, 094703.
- (8) Dong, Q.; Tian, W. Q.; Chen, D. L.; Sun, C. C. *Int. J. Hydrogen Energy* **2009**, *34*, S444–S448.
- (9) Georgiev, P. A.; Albinati, A.; Mojet, B. L.; Oliver, J.; Eckert, J. *J. Am. Chem. Soc.* **2007**, *129*, 8086.
- (10) Dietzel, P. D. C.; Georgiev, P. A.; Eckert, J.; Blom, R.; Straessle, T.; Unruh, T. *Chem. Commun.* **2010**, *46*, 1294.
- (11) Georgiev, P. A.; Albinati, A.; Eckert, J. *Chem. Phys. Lett.* **2008**, *449*, 182.
- (12) Robell, A. J.; Ballou, E. V.; Boudart, M. *J. Phys. Chem.* **1964**, *68*, 2748.
- (13) Srinivas, S. T.; Rao, P. K. *J. Catal.* **1994**, *148*, 470.
- (14) Conner, W. C.; Falconer, J. L. *Chem. Rev.* **1995**, *95*, 759.
- (15) Li, Y.; Yang, R. T. *J. Am. Chem. Soc.* **2006**, *128*, 8136.
- (16) Wang, L.; Yang, R. T. *Energy Environ. Sci.* **2008**, *1*, 268.
- (17) Cao, W.; Li, Y.; Wang, L.; Liao, S. J. *Phys. Chem. C* **2011**, *115*, 13829.
- (18) Wang, L.; Stuckert, N. R.; Chen, H.; Yang, R. T. *J. Phys. Chem. C* **2011**, *115*, 4793.
- (19) Lin, K.; Adhikari, A. K.; Chang, K.; Tu, M.; Lu, W. *Catal. Today* **2011**, *164*, 23.
- (20) Maseras, F.; Lledos, A.; Clot, E.; Eisenstein, O. *Chem. Rev.* **2000**, *100*, 601–636.
- (21) McGrady, G. S.; Guilera, G. *Chem. Soc. Rev.* **2003**, *32*, 383.
- (22) Morris, R. H.; Sawyer, J. F.; Shiralian, M.; Zubkoff, J. *J. Am. Chem. Soc.* **1985**, *107*, 5581.
- (23) Sluys, L. S. V. D.; Eckert, J.; Eisenstein, O.; Hall, J. H.; Huffman, J. C.; Jackson, S. A.; Koetzle, T. F.; Vergamini, P. J.; Caulton, K. G. *J. Am. Chem. Soc.* **1990**, *112*, 4831–4841.
- (24) Webster, C. E.; Gross, C. L.; Young, D. M.; Girolami, G. S.; A., J. S.; Hall, M. B.; Eckert, J. *J. Am. Chem. Soc.* **2005**, *107*, 15091.
- (25) Oldham, W. J.; Hinkle, A. S.; Heinekey, D. M. *J. Am. Chem. Soc.* **1997**, *119*, 11028.
- (26) Pons, V.; Conway, S. L. J.; Green, M. L. H.; Green, J. C.; Herbert, B. J.; Heinekey, D. M. *Inorg. Chem.* **2004**, *43*, 3475.
- (27) Janak, K. E.; Shin, J. H.; Parkin, G. *J. Am. Chem. Soc.* **2004**, *126*, 13054.
- (28) Li, S.; Hall, M. B.; Eckert, J.; Jensen, C. M.; Albinati, A. *J. Am. Chem. Soc.* **2000**, *122*, 2903–2910.
- (29) Riehl, J. F.; Pélissier, M.; Eisenstein, O. *Inorg. Chem.* **1992**, *31*, 3344.
- (30) Würger, A. *Z. Phys. B* **1989**, *76*, 65.
- (31) Hewson, A. C. *J. Phys. C* **1982**, *15*, 3855.
- (32) Limbach, H.-H.; Ulrich, S.; Gründemann, S.; Buntkowsky, G.; Sabo-Etienne, S.; Chaudret, B.; Kubas, G. J.; Eckert, J. *J. Am. Chem. Soc.* **1998**, *120*, 7929–7943.
- (33) Chai, J.-D.; Head-Gordon, M. *J. Chem. Phys.* **2008**, *128*, 084106.
- (34) Chai, J.-D.; Head-Gordon, M. *Phys. Chem. Chem. Phys.* **2008**, *10*, 6615.
- (35) Becke, A. D. *J. Chem. Phys.* **1993**, *98*, 5648.
- (36) Stephens, P.; Devlin, F.; Chabalowski, C.; Frisch, M. *J. Phys. Chem.* **1994**, *98*, 11623.
- (37) Tao, M.; Perdew, J. P.; Staroverov, V. N.; Scuseria, G. E. *Phys. Rev. Lett.* **2003**, *91*, 146401.
- (38) Hay, P. J.; Wadt, W. R. *J. Chem. Phys.* **1985**, *82*, 270.
- (39) Wadt, W. R.; Hay, P. J. *J. Chem. Phys.* **1985**, *82*, 284.
- (40) Hay, P. J.; Wadt, W. R. *J. Chem. Phys.* **1985**, *82*, 299.
- (41) Dunning, T. H.; Hay, P. J. In *Methods of Electronic Structure Theory*; Plenum Press: New York, 1977; Vol. 2.
- (42) Check, C. E.; Faust, T. O.; Bailey, J. M.; Wright, B. J.; Gilbert, T. M.; Sunderlin, L. S. *J. Phys. Chem. A* **2001**, *105*, 8111.
- (43) Frisch, M. J. et al. *Gaussian 09*, Revision A.1; Gaussian Inc.: Wallingford, CT, 2009.
- (44) Curl, R. F.; Hopkins, H. P.; Pitzer, K. S. *J. Chem. Phys.* **1968**, *48*, 4064.
- (45) Popović, Z.; Pavlović, G.; Roje, V.; Matković-Čalogović, D.; Došlić, N.; Leban, I. *Struct. Chem.* **2004**, *15*, 58.
- (46) Matanović, I.; Došlić, N. *J. Phys. Chem. A* **2005**, *109*, 4185.
- (47) Sorensen, D. *Tutorial: Implicitly Restarted Arnoldi/Lanczos Methods for Large Scale Eigenvalue Calculations*; Rice University: Houston, TX, 1995.
- (48) Lehoucq, R. B.; Sorensen, D.; Yang, C. D. *ARPACK User’s Guide: Solution of Large Scale Eigenvalue Problems with Implicitly Restarted Arnoldi Methods*; Rice University: Houston, TX, 1997.
- (49) Zhang, G.; Musgrave, C. B. *J. Phys. Chem. A* **2007**, *111*, 1554.
- (50) Braun, D.; Weiss, U. *Phys. B* **1994**, *202*, 264.
- (51) Scheurer, C.; Wiedenbruch, R.; Meyer, R.; Ernst, R. R.; Heinekey, D. M. *J. Chem. Phys.* **1997**, *106*, 1.
- (52) Special Issue: Symposium in Print on Tunnelling in Chemical and Biological Reactions. *J. Phys. Org. Chem.* **2010**, *23*, 559–710.
- (53) Kumar, P. P.; Marx, D. *Phys. Chem. Chem. Phys.* **2006**, *8*, 573.